Biochimica et Biophysica Acta 1788 (2009) 1033–1043

Contents lists available at ScienceDirect

Biochimica et Biophysica Acta

journal homepage: www.elsevier.com/locate/bbamem

Mechanisms of polyelectrolyte enhanced surfactant adsorption at the air–water interface

Patrick C. Stenger, Omer A. Palazoglu, Joseph A. Zasadzinski *

Department of Chemical Engineering, University of California, Santa Barbara, CA 93106-5080, USA

ARTICLE INFO

Article history:
Received 2 September 2008
Received in revised form 24 December 2008
Accepted 12 January 2009
Available online 27 January 2009

Keywords:
Competitive adsorption
Pulmonary surfactant
Inactivation
Inhibition
Electrostatics
Chitosan
Polycation

ABSTRACT

Chitosan, a naturally occurring cationic polyelectrolyte, restores the adsorption of the clinical lung surfactant Survanta to the air–water interface in the presence of albumin at much lower concentrations than uncharged polymers such as polyethylene glycol. This is consistent with the positively charged chitosan forming ion pairs with negative charges on the albumin and lung surfactant particles, reducing the net charge in the double-layer, and decreasing the electrostatic energy barrier to adsorption to the air–water interface. However, chitosan, like other polyelectrolytes, cannot perfectly match the charge distribution on the surfactant, which leads to patches of positive and negative charge at net neutrality. Increasing the chitosan concentration further leads to a reduction in the rate of surfactant adsorption consistent with an over-compensation of the negative charge on the surfactant and albumin surfaces, which creates a new repulsive electrostatic potential between the now cationic surfaces. This charge neutralization followed by charge inversion explains the window of polyelectrolyte concentration that enhances surfactant adsorption; the same physical mechanism is observed in flocculation and re-stabilization of anionic colloids by chitosan and in alternate layer deposition of anionic and cationic polyelectrolytes on charged colloids.

1. Introduction

Monolayer films of lung surfactant (LS) line the alveolar air–water interface and lower the interfacial tension in the lungs, thereby minimizing the work of breathing [1,2]. The surface tension control imposed by LS can be compromised during acute respiratory distress syndrome (ARDS), which afflicts 140,000 people annually in the US with a 40% mortality rate [3–5]. The clinical similarities between ARDS and neonatal RDS have led to the hypothesis that the same lack of functional surfactant that causes NRDS might be a common factor. Surfactant replacement therapy is the primary treatment for pediatric patients with NRDS [6–8], but there has been less success with ARDS and other forms of lung injury [9]. A contributing factor to the development and severity of ARDS may be the elevated serum and inflammatory protein levels in the bronchial and alveolar fluid of ARDS patients [2,10–13]. *In vitro*, there is an ARDS-like depression of LS activity when serum proteins are added to a LS-covered interface [14,15], LS is added to a serum-covered interface [16,17] or both LS and serum proteins are presented simultaneously [18].

A necessary [16,17,19–21], but not sufficient condition [5,22], for surfactant activity is to have sufficient LS transported to the interface from the type II cells that line the alveoli. Previous work has shown that the competitive adsorption of serum proteins to the air–water interface can inhibit the adsorption of lung surfactant, leading to poor surfactant performance [14–18,20,21,23,24]. Many serum proteins are surface-active and have a surface pressure, Π, ($\Pi = \gamma_w - \gamma$; γ_w is the surface tension of a clean air–water interface, 72 mN/m, and γ the measured surface tension) that is a logarithmic function of protein concentration up to a saturation concentration, which is ~1 mg/mL for albumin [15,25]. The surface pressure at the saturation concentration for albumin and many other serum proteins is between 18 and 25 mN/m (γ ~47–54 mN/m) [15,25], which is much lower than Π~70 (γ near zero) required for proper respiration.

Albumin (as well as any other surface-active material) adsorbed at the alveolar air–water interface induces an energy barrier that inhibits surfactant transport to the interface, thereby slowing surfactant adsorption [16–18,21,26,27]. The physical processes governing surfactant transport to an interface are identical to those that determine colloid stability; the energy barrier that limits surfactant adsorption in the presence of serum proteins is directly analogous to those that lead to colloid stability against aggregation [17,20,21]. Hence, it should not be surprising that many of the same additives used to lower the energy barrier and promote colloid aggregation [28–35] lead to enhanced surfactant adsorption. The first examples of the analogy between colloid stability and surfactant adsorption came from observations that adding non-ionic hydrophilic polymers such as polyethylene glycol (PEG) and dextran [18,23,36–38] or anionic polymers such as hyaluronic acid [39,40] to clinical surfactants improved lung function of animals over that of surfactant alone. This improved lung function correlated well with enhanced surfactant adsorption to an albumin-covered air–water interface *in vitro*, as well

* Corresponding author. Tel.: +1 805 893 4769; fax: +1 805 893 4731.
E-mail address: gorilla@engineering.ucsb.edu (J.A. Zasadzinski).

0005-2736/$ – see front matter © 2009 Elsevier B.V. All rights reserved.
doi:10.1016/j.bbamem.2009.01.006

as flocculation of the lung surfactant particles in the suspension [17,19–21,27]. Both the enhanced adsorption to the air–water interface [41] and flocculation of the surfactant aggregates in suspension [42] could be explained as originating from the depletion attraction that entropically pushes the surfactant aggregates toward the interface and toward each other, thereby overcoming an albumin-induced energy barrier [21].

This albumin-induced energy barrier to surfactant adsorption is primarily electrostatic [19,26]; a double-layer repulsion arises due to the negative lipids in lung surfactant and the net negative charge on albumin (and other surface-active serum proteins) at the interface [28]. Classical methods of manipulating the double-layer repulsion in colloids using electrolytes have similar, predictable effects on surfactant adsorption. Decreasing the electrolyte concentration below physiological levels increases the Debye length and the magnitude and range of the double layer repulsion, which eliminates surfactant adsorption even in the presence of the polymer-induced depletion attraction [19]. Conversely, increasing the bulk electrolyte concentration well above physiological levels restores surfactant adsorption in the presence of albumin without the need for added polymer [19,26].

The third common method of stabilizing or flocculating charged colloids, which has a long history in wastewater treatment, mineral processing, ceramics manufacture and papermaking, relies on adding oppositely charged *polyelectrolytes* [30–35]. Cationic polyelectrolytes, such as chitosan, are particularly useful, as they are oppositely charged to the negatively charged surfaces common to biological systems. In analogy to its effects on colloid stability, chitosan improves the performance of lung surfactant *in vitro* [24,43]. Here we show that only 0.001 mg/mL chitosan is able to reverse albumin-induced surfactant inhibition to the same extent as ~10 mg/mL 10 kDa PEG [16,17,20,21,27] or ~1 mg/mL 1240 kDa hyaluronic acid [16,21] under otherwise identical conditions. These chitosan concentrations are much too low to induce a depletion attraction, which is proportional to the polymer volume fraction [21,41,42,44]. However, unlike PEG or HA, increasing the chitosan concentration above optimal causes surfactant inhibition to re-occur. The chitosan concentration range that reverses inhibition is roughly that necessary to neutralize the negative charge on a given concentration of Survanta. This charge neutralization mechanism is identical to that observed in flocculation of colloidal particles by chitosan and other cationic polyelectrolytes [30–35]. At the chitosan concentration is increased, the net negative charge in the double-layer surrounding both Survanta and albumin are neutralized, leading to an elimination of the electrostatic repulsion between the Survanta and the albumin-covered interface [30–35]. However, as is often the case for polyelectrolytes, increasing the polymer concentration further leads to additional chitosan binding to the surfaces resulting in an over-compensation of the surface charge. This re-establishes an electrostatic energy barrier [30–35] and leads to a decrease in surfactant adsorption. The same physical mechanism is observed in flocculation and re-stabilization of anionic colloids by chitosan [30–32] and in alternate layer deposition of anionic and cationic polyelectrolytes on charged colloids [33]. These results confirm the fundamental importance of electrostatics in determining the competitive adsorption of surfactant as well as the analogy between surfactant adsorption and colloid stability.

2. Methods

Survanta (Abbott Laboratories, Columbus, Ohio) was a generous gift of the Santa Barbara Cottage Hospital nursery. Survanta is an organic extract of minced bovine lungs that has been fortified with dipalmitoylphosphatidylcholine (DPPC), tripalmitin and palmitic acid. Survanta contains 80–90% wt. phosphatidylcholine, of which, ~70% wt. is saturated DPPC and about 10% wt. palmitic acid [45,46]. The preparation contains approximately 7% wt. negatively charged phospholipids including phosphatidylglycerol and phosphatidylserine giving the Survanta aggregates a net negative charge [46]. Survanta has minimal amounts of SP-B, 0.04–0.13% wt. but close to native amounts of SP-C, 0.9–1.65% wt. [45,47,48]. Both SP-B and SP-C are cationic, which partially compensates the negative charge on the lipids. Like other natural products, Survanta can vary somewhat from batch to batch due to variations in extraction and purification as well as variations in the source materials. Survanta and other clinical lung surfactants form multi-micron bilayer aggregates in buffered saline solution [47]. Bovine serum albumin, 75–85% deacetylated chitosan (~50–190 kDa) and palmitic acid (PA) were obtained from Sigma (St. Louis, MO) and used as received.

Isotherms were recorded at 25 °C (no significant changes are seen from 23–37 °C [49]) using a custom stainless steel ribbon trough (Nima, Coventry, England) designed to minimize film leakage at high surface pressures (low surface tensions). Surface pressure was monitored during compression and expansion using a filter paper Wilhelmy plate. The trough had a surface area of 130 cm^2; a subphase volume of 150 mL and a typical compression/expansion cycle took 8 min (~0.42 cm^2/s). All water used in experiments was obtained from a Millipore Gradient System (Billerica, MA) and had a resistivity of 18.2 MΩ/cm. The buffered-saline subphase contained 150 mM NaCl, 2 mM $CaCl_2$, 0.2 mM $NaHCO_3$ in addition to the stated concentrations of albumin and chitosan. For experiments with chitosan, the solution pH was reduced to ~2.0 with 1 M HCl until a clear solution was obtained after adding chitosan; the pH of the solution was then raised to ~5.5 with 1 M NaOH. The subphase pH for all experiments was held at ~5.5; as the pK_a for chitosan is ~6.5, ~90% of the amine groups are positively charged. For an average chitosan molecular weight of 120 kDa with ~80% of the repeat units containing an amine group, this yields ~500 positive charges per molecule.

To initiate each experiment, a saline-buffered subphase containing albumin and chitosan was added to the Langmuir trough and allowed to equilibrate for 10 min. For albumin containing subphases, the surface pressure gradually increased to ~18 mN/m consistent with the well-established relation between surface activity and albumin concentration [15,25]. Chitosan in buffer showed no surface activity (Fig. 3). For all experiments, Survanta was diluted in a standard buffer (150 mM NaCl, 2 mM $CaCl_2$, 0.2 mM $NaHCO_3$, pH = 7.0) to a lipid concentration of 2 mg/mL and was deposited as microliter drops from a syringe by touching the drop to the air–water interface of the open trough. The drops passed through the interface into the subphase adjacent to the interface; surfactant adsorption from the subphase was followed by labelling the Survanta with 1 mol% of the fluorescent lipid Texas Red-DHPE (Invitrogen, Eugene, OR). The drops did not spread appreciably at the interface and essentially all of the Survanta adsorbed from the subphase [17]. The subphase was not stirred and the first compression began 20 min after deposition of a fixed quantity of Survanta. The amount of Survanta chosen for the inhibition experiments, 800 μg, was such that collapse would occur at about 50% trough compression in the absence of albumin; the same amount of surfactant was used in all subsequent experiments.

A Nikon Optiphot optical microscope (Nikon, Tokyo, Japan) with either a 10× or 50× extra long working distance objective designed for fluorescent light [50] was positioned above the trough. Full-length movies and individual frames were recorded directly to computer (Moviestar, Mountain View, CA). Contrast in the images was due to segregation of 1% mol fluorescent lipid Texas Red-DHPE (Invitrogen, Eugene, OR) between the liquid expanded and condensed phases which causes the Survanta monolayer to have a light gray–dark gray coexistence in images [17,49]. Larger aggregates of Survanta have significantly more dye than the monolayer film and appear bright white, leading to an overall mottled texture for the surfactant film. The albumin was not labeled, does not fluoresce and appears black in the images.

3. Results

Fig. 1a shows a typical compression–expansion cyclic isotherm for 800 μg of Survanta adsorbing to a buffered-saline interface. The isotherm traces over itself on subsequent cycles and on compression exhibits a characteristic shoulder at $\Pi \sim 45$ mN/m and collapse plateau at $\pi_{max} \sim 69$ mN/m where the film begins to "collapse" and form cracks and folds [17,49,51,52]. Film collapse determines the minimum surface tension possible for a given surfactant. The hysteresis between compression and expansion cycles is typical of Survanta and other clinical and natural lung surfactant isotherms [2,53] Expanding the interface after monolayer collapse leads to a rapid drop in surface pressure to a minimum of 5–10 mN/m which is maintained until compression is resumed. There is no significant change in the Survanta isotherms from 23–37 °C [49].

Conversely, when the same amount of Survanta (800 μg) is deposited onto a subphase containing 2 mg/mL albumin (Fig. 1b, black curve), the surface pressure does not increase above 42 mN/m even at the smallest trough area. The concentration of albumin used here are above the ~1 mg/ml saturation concentration at which the albumin surface pressure no longer increases with concentration [15,25]. Reports of the average albumin concentrations in the alveolar fluid of ARDS patients and healthy patients vary widely. Estimates range from 0.5 mg/mL for ARDS patients compared to 0.03 mg/mL for healthy patients [13] to 25 mg/mL for ARDS patients compared to 5 mg/mL for healthy patients [12].

The characteristic shoulder and collapse plateau seen upon compression in Fig. 1a cannot be reached with albumin in the subphase at this Survanta concentration; a five fold increase in Survanta concentration yields only a partial recovery of these features [17]. The minimum surface pressure (~15 mN/m) during expansion in Fig. 1b is higher than Fig. 1a and is set by the re-adsorption of albumin to the interface at its saturation surface pressure [15]. Both the compression and expansion isotherms are not different than that of albumin alone (Fig. 1b, red curve), indicating that albumin has excluded the Survanta from the interface (see Fig. 4b). Albumin at these compression rates can significantly exceed its equilibrium surface pressure of ~18 mN/m.

Fig. 1c shows Survanta (800 μg) deposited onto a subphase containing 2 mg/mL albumin and 0.005 mg/mL chitosan; the isotherm resembles Survanta on a clean interface (Fig. 1a) by the second compression-expansion cycle. Subphase chitosan does not alter the surface pressure at which the characteristic shoulder ($\Pi \sim 45$ mN/m) and collapse plateau ($\Pi_{max} \sim 69$ mN/m) occur but rather enhances the adsorption of surfactant to the interface and the displacement of albumin from the interface. The major change between Fig. 1a and c is that the minimum surface pressure during expansion never drops below ~15 mN/m (which is the equilibrium surface pressure of the albumin) when albumin is present (see Fig. 1b) [15]. The restoration of the Survanta isotherm (Fig. 1a) during subsequent compression cycles in Fig. 1c shows that the rate of surfactant adsorption to the interface is sufficient to prevent any

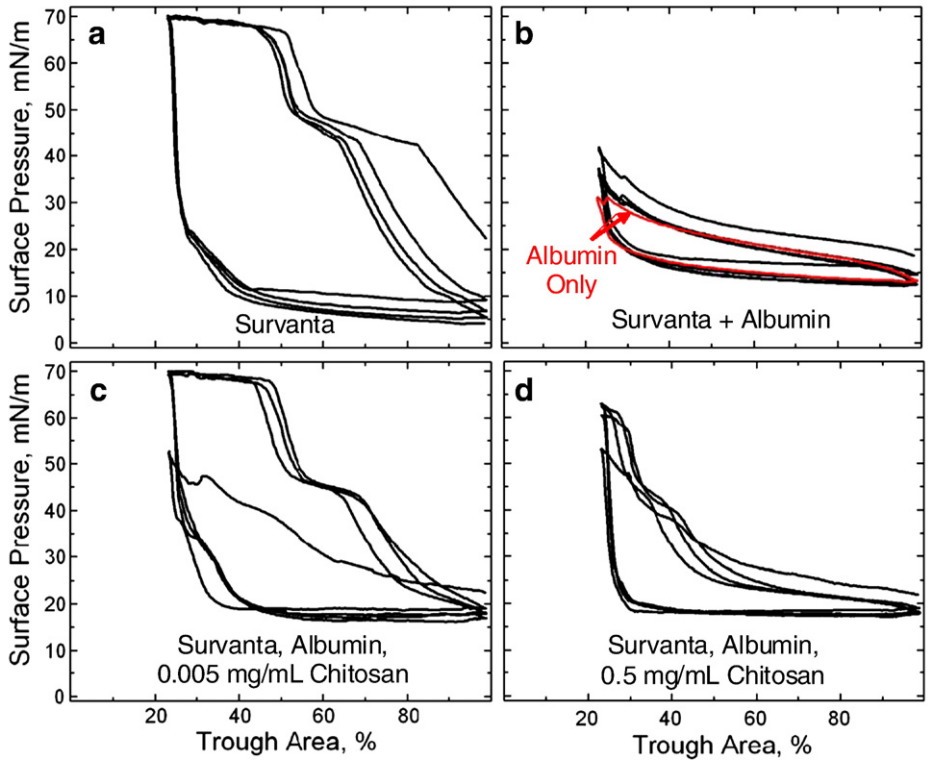

Fig. 1. (a) Cyclic isotherms of 800 μg Survanta deposited from an aqueous buffer onto a saline-buffered subphase containing no albumin or chitosan. On compression, the isotherm exhibits a characteristic shoulder at 45 mN/m and a collapse plateau at $\Pi_{max} \sim 69$ mN/m. On expansion, the surface pressure drops rapidly, reaching a minimum surface pressure of ~5–10 mN/m until compression is resumed. (b) Black curve: 800 μg Survanta added to a saline-buffered subphase containing 2 mg/mL albumin. The characteristic shoulder and collapse plateau on compression seen in (a) cannot be reached with albumin in the subphase regardless of the compression. Red curve: The isotherm of a subphase containing 2 mg/mL albumin, with no added Survanta or chitosan. The two curves trace over each other, indicating that the interfacial film is dominated by albumin and that Survanta is not adsorbing to the interface. (c) 800 μg Survanta deposited on a subphase containing 2 mg/mL albumin and 0.005 mg/mL chitosan. By the second compression cycle, the characteristic shoulder and collapse plateau have been restored at similar trough areas as in (a) showing that the presence of 0.005 mg/mL chitosan completely reverses the surfactant adsorption inhibition. The only difference with the Survanta isotherms in panel a is that the minimum surface pressure in the presence of albumin never drops below about 15 mN/m on full expansion, which corresponds to the equilibrium spreading pressure of the albumin. (d) 800 μg Survanta deposited on a subphase containing 2 mg/mL albumin and 0.5 mg/mL chitosan. At high trough areas, the isotherm resembles that of albumin (panel b), while at low trough areas, the characteristic shoulder is evident as in panel a. However, the isotherm only reaches a surface pressure of ~60 and the collapse plateau does not form at the limiting compression. This indicates that the increased chitosan concentration decreases surfactant adsorption compared to panel c.

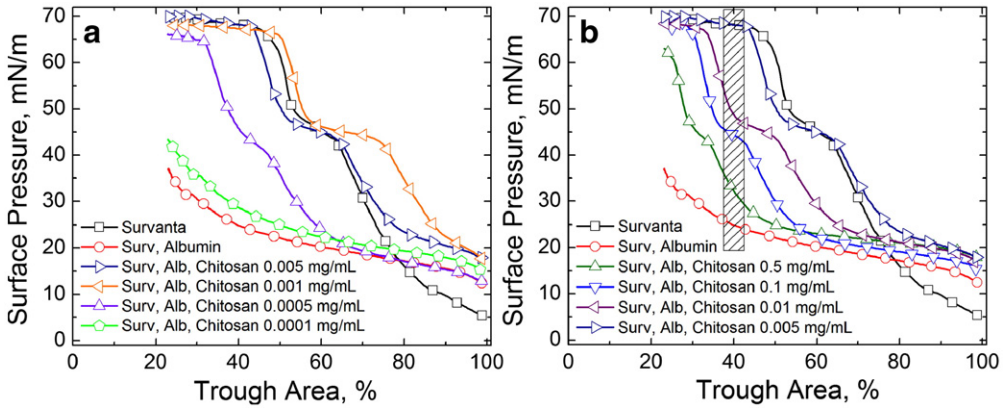

Fig. 2. Fourth cycle compression isotherms of 800 μg Survanta on a saline buffered subphase containing albumin (2 mg/mL when present) and the stated chitosan concentrations. (a) □ Survanta; ○ Survanta–albumin; ▷ Survanta–albumin with 0.005 mg/mL chitosan, ◁ Survanta–albumin with 0.001 mg/mL chitosan; △ Survanta–albumin with 0.0005 mg/mL chitosan; ⬠ Survanta–albumin with 0.0001 mg/mL chitosan. In this concentration regime, increasing chitosan concentration yields increasing surfactant adsorption. From Table 1, charge neutralization of the Survanta and albumin is reached between 0.0005–0.005 mg/mL chitosan. Note that for .001 mg/mL chitosan, more Survanta adsorbs (isotherm shifted to larger trough areas) than the control Survanta on a clean subphase. (b) □ Survanta; ○ Survanta–albumin; △ Survanta–albumin–chitosan 0.5 mg/mL, ▽ Survanta–albumin–chitosan 0.1 mg/mL; ◁ Survanta–albumin–chitosan 0.01 mg/mL; ▷ Survanta–albumin–chitosan 0.005 mg/mL. For chitosan concentrations greater than that necessary for charge neutralization (Table 1), surfactant adsorption decreased. The shaded area denotes the trough area over which the surface pressure was averaged for each chitosan concentration to obtain the surfactant relative adsorption plotted in Fig. 6.

appreciable albumin re-adsorption. When Survanta (800 μg) is spread on a subphase containing 0.005 mg/mL chitosan with no albumin, the isotherm is identical to Fig. 1a (data not shown); this shows that the chitosan is primarily enhancing the adsorption of Survanta to the interface with minimal alterations of the surfactant properties.

However, further increases in chitosan concentration led to increasingly poor Survanta performance. Fig. 1d shows that Survanta (800 μg) deposited onto a subphase containing 2 mg/mL albumin and 0.5 mg/mL chitosan exhibits an isotherm that is intermediate between Survanta (Fig. 1a) and Survanta–albumin (Fig. 1b). Here the isotherm only reaches a maximum surface pressure of $\Pi \sim 62$ mN/m on full compression (ratio of 4:1 compared to the 2:1 in Fig. 1a, c) and the characteristic shoulder at $\Pi \sim 45$ mN/m occurs at a significantly lower trough area than Survanta (~35% vs. ~60%). The increased chitosan concentration results in less surfactant adsorption to the interface than for the lower chitosan concentration (Fig. 1c). For the depletion attraction induced increase in Survanta adsorption, surfactant adsorption increased exponentially with polymer concentration up to a saturation concentration; surfactant adsorption did not decrease [17].

Fig. 2a and b show the effect of varying chitosan concentrations on Survanta (800 μg) deposited onto a subphase containing 2 mg/mL albumin; for clarity, only the fourth cycle compression is shown for each isotherm. Fig. 2a shows that a chitosan concentration of 0.0001 mg/mL (Fig. 2a, pentagons) reaches a maximum surface pressure of 45 mN/m, similar to the Survanta–albumin isotherm (Fig. 2a, circles). Increasing the chitosan concentration to 0.0005 mg/mL (Fig. 2a, up-triangles) restores the characteristic shoulder and collapse plateau at a smaller trough area than Survanta on a clean interface (Fig. 2a, squares), indicating less total surfactant adsorption [17]. For chitosan concentrations of 0.001–0.005 mg/mL (Fig. 2a, left-triangles, right-triangles), the characteristic shoulder and collapse plateau occur at similar trough areas as Survanta, indicating an equivalent amount of total surfactant adsorption. In fact, more Survanta adsorbs for the optimal chitosan concentration of .001 mg/mL than on a clean interface — the isotherm is shifted to larger trough areas at all surface pressures. Note that the surface pressures of the characteristic shoulder and the collapse pressure of the Survanta does not change with chitosan concentration, once adsorption has been restored.

Fig. 2b shows that increasing the chitosan concentration above this optimum value yields a gradual decrease in surfactant adsorption. Increasing chitosan concentrations shift the characteristic shoulder and collapse plateau to a lower trough area without altering the surface pressures at which they occur. While surfactant adsorption at 0.5 mg/mL (Fig. 2b, up triangles) is decreased from the optimum chitosan concentration (0.005 mg/mL, up-triangles), the isotherm is still representative of an interface with Survanta compared to the isotherm of albumin alone (Fig. 1b).

Fig. 3 shows the fourth cycle isotherms from subphases containing albumin and/or chitosan in the absence of Survanta. Chitosan itself is not surface active (Fig. 3, triangles) at these concentrations; similar results are found for concentrations ranging from 0.0001–0.5 mg/mL. The 2 mg/mL albumin isotherm (Fig. 3, squares) is unchanged by 0.1 mg/mL chitosan (Fig. 3, circles); the curves differ by no more than 3 mN/m over the entire cycle. Albumin reaches a maximum surface pressure of ~31 mN/m upon compression and a minimum surface pressure of ~13 mN/m upon expansion indicating that its adsorption and surface activity are unchanged by chitosan. Saline buffer subphases containing 0.0005–0.5 mg/mL chitosan and 2 mg/mL albumin are optically clear, putting an upper limit on the aggregation in the bulk. Other reports show that chitosan does not significantly increase the turbidity of an albumin solution at salt concentrations

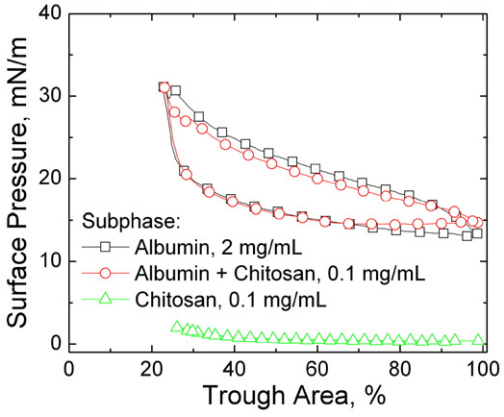

Fig. 3. Fourth cycle compression isotherms of subphases containing albumin and/or chitosan without Survanta. □ 2 mg/mL albumin; ○ 2 mg/mL albumin–0.1 mg/mL chitosan; △ 0.1 mg/mL chitosan. Albumin is surface active while chitosan is not; chitosan addition does not change the albumin isotherm. Compressing the albumin film increases the surface pressure from about 15 mN/m to a maximum of about 30 mN/m; expanding the albumin film shows a similar hysteresis to the Survanta monolayer as the surface pressure rapidly drops to <20 mN/m and is roughly constant during the expansion. This minimum surface pressure is likely set by adsorption of albumin from solution.

used in this work, confirming that chitosan does not cause large scale aggregation of the albumin in solution [54].

Fig. 4a shows a fluorescence image of the air–water interface after Survanta adsorption ($\Pi = 43$ mN/m) on a saline buffer subphase. Survanta (doped with 1% mol Texas Red-DHPE) adsorbs to the interface as a mixture of monolayers (mottled light gray and dark gray) typical of a phase separated lipid/protein monolayer along with bright, three-dimensional aggregates that appear to be attached to the

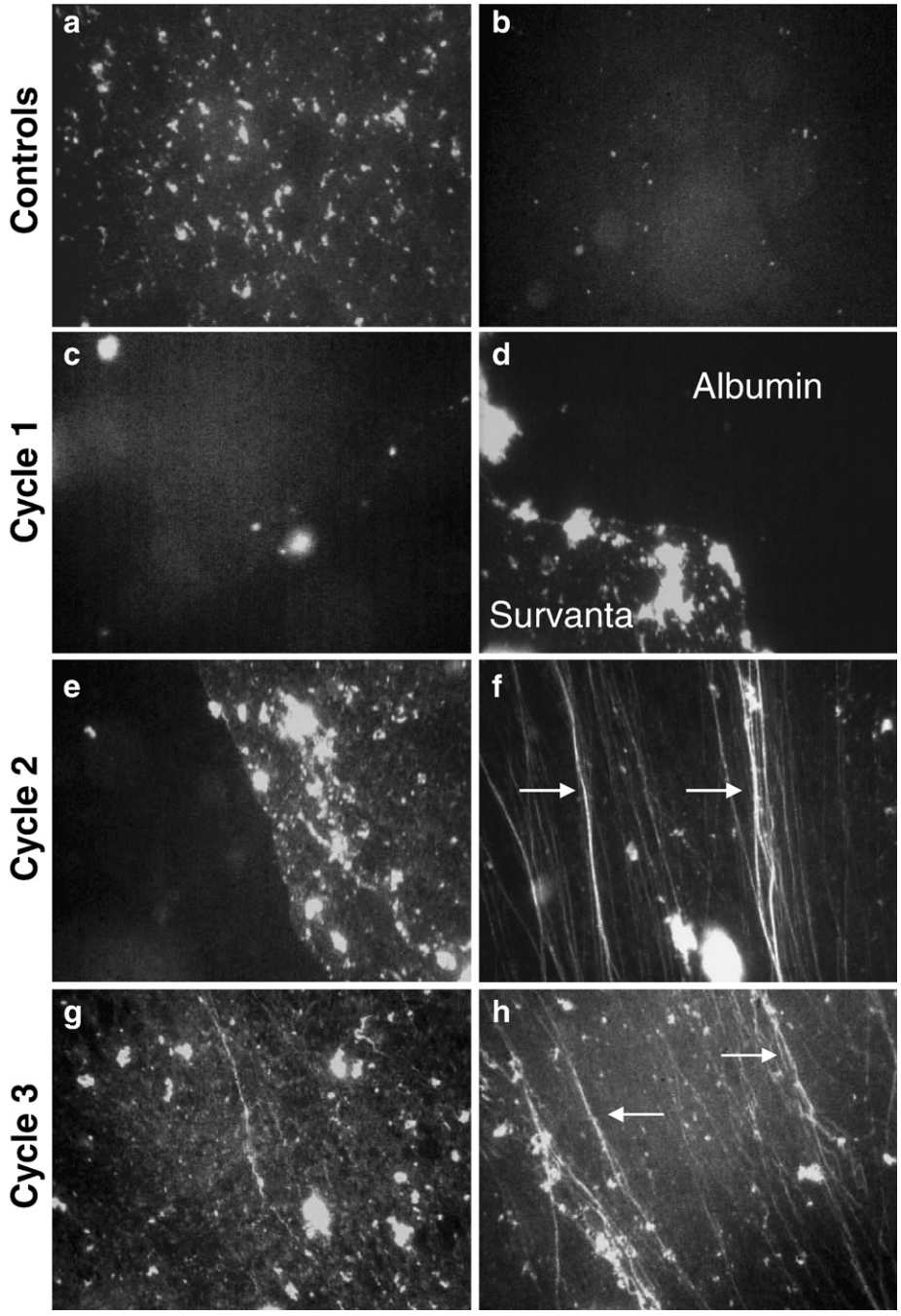

Fig. 4. Fluorescence images of 800 μg Survanta (doped with 1% mol Texas Red DHPE) spread at varying subphase compositions. The albumin was not labeled, does not fluoresce and appears black in the images. Images are 1023 μm by 789 μm; all images are from the compression part of the isotherm. (a) Survanta on a clean, buffered subphase at $\pi = 43$ mN/m. The image shows the mottled texture typical of a phase separated lipid/protein monolayer. The bright spots are Survanta aggregates partially adsorbed to the interface and partially in solution. (b) Survanta on a subphase containing 2 mg/mL albumin at $\pi = 25$ mN/m. The isolated bright spots on a homogeneous black background shows that Survanta aggregates come close to the interface, but cannot spread due to the albumin film at the interface. The albumin effectively prevents Survanta from adsorbing to the interface. The remaining images show Survanta on a subphase containing 2 mg/mL albumin and 0.005 mg/mL chitosan during successive compression/expansion cycles. First cycle: (c) $\pi = 25$ mN/m. The isolated bright spots on a homogenous black background shows that Survanta aggregates cannot easily spread due to the albumin film at the interface. (d) $\Pi = 54$ mN/m. Survanta breaks through the interface; extended (>1000 μm) immiscible Survanta (mottled gray) and albumin (black) domains coexist on the interface. The surface pressure needed to remove albumin from the interface is much greater than the 15–20 mN/m equilibrium spreading pressure of albumin. Second cycle: (e) $\pi = 43$ mN/m. Continued coexistence between Survanta and albumin domains (f) $\pi = 69$ mN/m. At the collapse plateau, only Survanta is present in the film; the images are dominated by the cracks and folds (arrows) typical of monolayer collapse. As suggested by a recent theoretical model, the collapse folds are roughly parallel to each other and are perpendicular to the compression direction [52]. Several smaller folds have coalesced into the brighter white, larger folds at the arrows, also as suggested by theory [52]. Third cycle: (g) $\pi = 43$ mN/m. Once albumin is removed from the interface, the film morphology is identical to Survanta on a buffered subphase and albumin does not re-adsorb to the interface under these conditions. (h) $\pi = 69$ mN/m. The arrows indicate brighter collapse cracks and folds at which smaller folds have coalesced [52].

interface [17,19,20,49]. This characteristic mottled texture is found at all surface pressures. In contrast, Fig. 4b shows that fluorescence images of Survanta spread on a subphase containing 2 mg/mL albumin ($\pi = 25$ mN/m) consists of isolated, out-of-focus lighter gray regions with an overall dark homogeneous background [17,19,20]. Albumin does not fluoresce and appears dark and featureless in the images. Fig. 4b shows that Survanta cannot reach the interface to form a monolayer; the interface is dominated by albumin. The surface pressure does not significantly increase (Fig. 1b) on compression as only albumin is present at the interface.

Fig. 4c–h show Survanta deposited onto a subphase containing 2 mg/mL albumin and 0.005 mg/mL chitosan during successive compression/expansion cycles; the mottled Survanta texture gradually displaces the darker albumin texture from the interface. The albumin and Survanta do not appear to be miscible at the interface; rather, a Survanta front displaces the albumin from the interface (see Movies in Supplemental Materials). Images from the first cycle at low surface pressure (Fig. 4c, $\pi = 25$) show a homogeneous black, albumin-covered interface with limited out-of-focus light gray patches, indicating that the Survanta aggregates cannot reach the

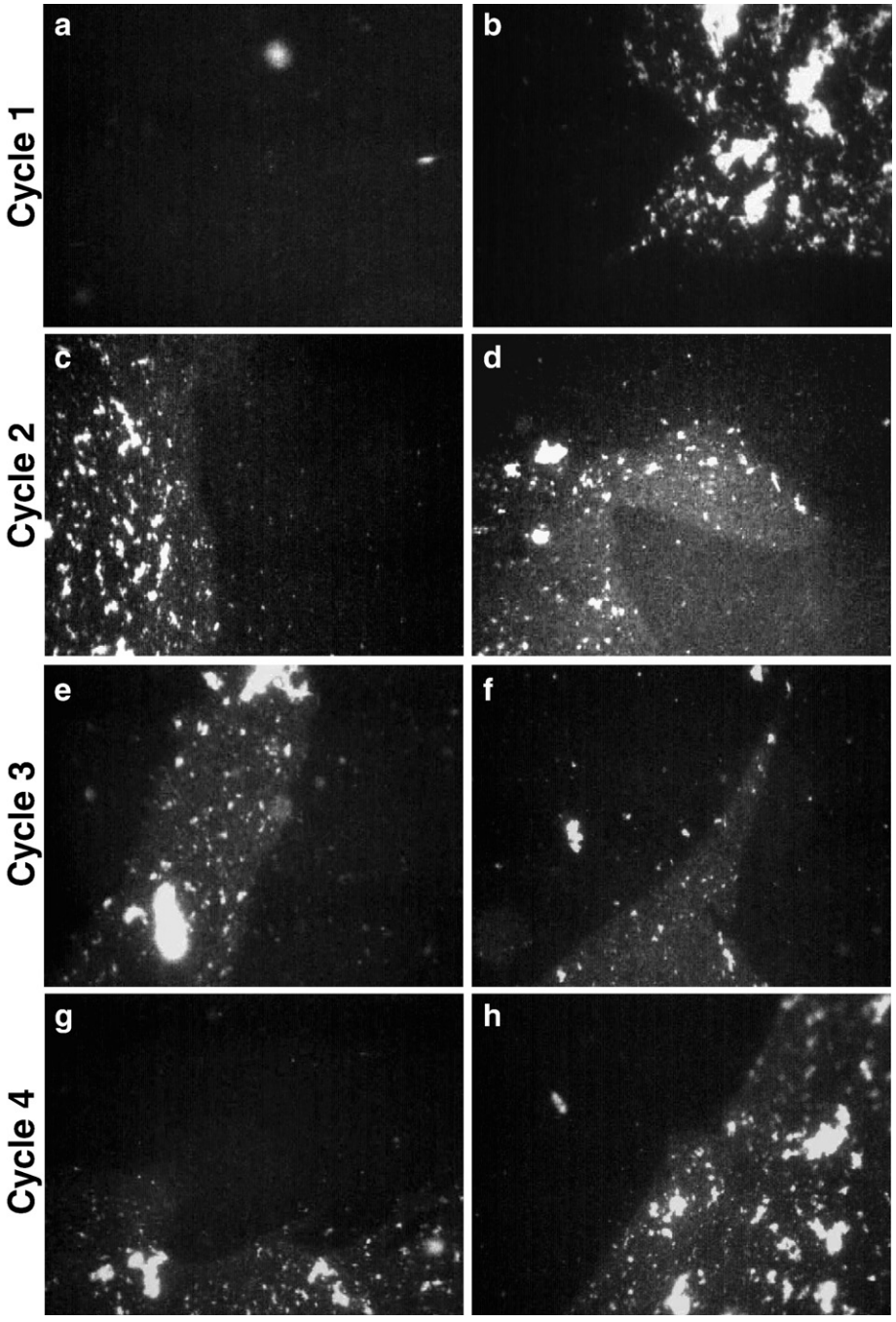

Fig. 5. Fluorescence images of 800 μg Survanta spread on a saline buffered subphase containing 2 mg/mL albumin and 0.5 mg/mL chitosan. Images are 1023 μm by 789 μm. First cycle (a) $\pi = 25$ mN/m during compression. The black homogenous background dominates the interface as the albumin prevents the Survanta from spreading as a monolayer. (b) $\pi = 18$ mN/m during expansion. Survanta breaks through the interface; extended (>1000 μm) immiscible Survanta (mottled gray) and albumin (black) domains coexist on the interface. Second cycle (c) $\pi = 21$ mN/m during compression. (d) $\pi = 18$ mN/m during expansion. The albumin and Survanta domains coexist during the compression and expansion cycle. Third cycle (e) $\pi = 21$ mN/m during compression. (f) $\pi = 18$ mN/m during expansion. Albumin and Survanta domains coexist on the interface. Fourth cycle (g) $\pi = 24$ mN/m during compression. (h) $\pi = 18$ mN/m during expansion. Albumin remains on the interface through the fourth compression and expansion cycle. Apparently a sufficient quantity of Survanta does not adsorb to completely expel the albumin from the interface.

surface to spread as a monolayer. Fluorescence movies of the interface indicate that in the presence of chitosan, Survanta adsorbs when the bright aggregates near the interface adsorb to the albumin-covered interface and are explosively disrupted (see Movie #1 in Supplemental Materials). Images from the first cycle maximum surface pressure (Fig. 4d, $\pi = 54$) show that Survanta has broken through the albumin film; there is coexistence between the Survanta (mottled bright texture) and albumin (black) with a well-defined interface between the materials. The coexistence between the extended (>1000 μm) interfacial domains of Survanta and albumin continues through the second cycle compression (Fig. 4e, $\pi = 43$); albumin remains on the interface well above its equilibrium surface pressure of ~20 mN/m. However, Survanta can maintain a much higher dynamic surface pressure on compression than the albumin and eventually forces all of the albumin from the interface (see Movie #2 in Supplemental Materials) at surface pressures of $\Pi \sim 60$ mN/m [17,19,20]. To generate this higher dynamic surface pressure, additional Survanta likely adsorbs from the bright aggregates attached to the interface to occupy the new interface created as the trough expands. Images of the second cycle collapse plateau (Fig. 4f, $\pi = 69$) show only Survanta and are dominated by the cracks and folds (arrows) typical at monolayer collapse [17,49]. As suggested by a recent theoretical model, the collapse folds in Fig. 4f are roughly parallel to each other and are perpendicular to the compression direction [52]. Several smaller folds have coalesced into the brighter white, larger folds at the arrows, also as suggested by this theory [52]. On the third cycle compression, the mottled Survanta texture similar to Fig. 4a is seen exclusively at all surface pressures (Fig. 4g, $\pi = 43$) and the system again forms a collapse plateau with the associated cracks and folds (Fig. 4h, $\pi = 69$). The chitosan does not appear to alter the morphology or phase behavior of the Survanta, the chitosan primarily acts to enhance Survanta adsorption.

Fig. 5 shows Survanta deposited onto a subphase containing 2 mg/mL albumin and 0.5 mg/mL chitosan during successive compression/expansion cycles; here Survanta breaks through interface but never completely displaces the albumin. Similar to 0.005 mg/mL chitosan, images from the first cycle compression (Fig. 5a, $\pi = 25$) show a homogeneous black, albumin-covered interface while images from the first cycle expansion (Fig. 5b, $\pi = 18$) show that Survanta has broken through the albumin film. During the second and subsequent cycles, images from the compression and expansion parts of the isotherm show a continued coexistence of Survanta and albumin domains; albumin remains on the interface through the fourth cycle. This behavior is consistent with the isotherm in Fig. 1d, which shows that the film does not achieve the sufficiently high surface pressure needed to expel the albumin from the interface. While 0.5 mg/mL chitosan enhances surfactant adsorption enough to initially *break through* the albumin interface, additional surfactant does not adsorb on expansion of the film to sufficiently raise the surface pressure to entirely *eliminate* the albumin from the interface. For both chitosan concentrations (Fig. 4c–h, Fig. 5), the images show the Survanta morphology similar to the control (Fig. 4a) whether the surfactant fully displaces or only partially displaces the albumin on the interface. Chitosan does not change the monolayer microstructure but rather enhances surfactant adsorption to the interface. A contributing effect may be that the adsorbed chitosan stabilizes the Survanta in the aggregate form; chitosan adsorbed to giant unilamellar vesicles stabilized the spherical bilayer structure against changes in pH or osmotic pressure [55] that completely disrupted unprotected vesicles.

4. Discussion

Comparison of fluorescence images and isotherms of Survanta adsorption to clean interfaces [49], or albumin-covered interfaces with chitosan, electrolyte [19] or PEG in the subphase [17,20] shows the Survanta morphology and organization at the interface are the same, confirming that all of these treatments enhance Survanta transport to the interface while leaving the surfactant essentially unchanged. For all methods of enhancing adsorption [17,19,20], the images show that competitive adsorption process is similar:

(1) Albumin initially occupies the entire interface; the smaller size of albumin compared to Survanta aggregates promotes faster diffusion to the interface.
(2) Survanta breaks through the albumin film during cycling and coexists with albumin in discrete domains on the interface.
(3) Sufficient Survanta adsorbs such that the surface pressure is raised to ~60 mN/m during compression, completely expelling the albumin from the interface.
(4) Survanta prevents subsequent albumin adsorption to the interface; the fluorescence images show behavior typical of Survanta on a clean subphase including cracks and folds at the collapse plateau.

Albumin expulsion from the interface (step 3) only occurs completely only over an optimal chitosan concentration range (0.001–0.005 mg/mL) while higher and lower chitosan concentrations do not fully expel the albumin from the interface. Similarly, at sub-optimal concentrations of simple electrolytes and PEG, Survanta can break through the albumin layer in patches, but cannot completely displace albumin from the interface. Higher concentrations of PEG or electrolyte, however, does allow Survanta to entirely expel albumin [17,19,20].

The competitive adsorption of lung surfactant and albumin, like colloid stability, is an example of a kinetically hindered equilibrium. The surface pressure, Π, is the negative derivative of the energy, Φ, with respect to the interfacial area, A: $\Pi = -\left(\frac{\partial \Phi}{\partial A}\right)_n$ [56]. Hence, at equilibrium, lung surfactant should always displace albumin at an air–water interface; the equilibrium surface pressure of LS (~45 mN/m) is much greater than that of albumin (~20 mN/m). Similarly, most apparently stable colloidal dispersions should aggregate at equilibrium [28]. The interactions between colloidal particles are a combination of the van der Waals/London dispersion attraction [57] and the double-layer electrostatic repulsion [28] which gives the functional form of $\Phi(r)$ between two colloids of radius, a, at a separation, r, surface potential, ψ_s, and ion concentration, n_i via the Debye length, $\kappa^{-1} = \left[(\varepsilon\varepsilon_0)k_B T/\left(e^2 \sum_i z_i^2 n_i\right)\right]^{1/2}$:

$$\Phi(r) = 32\pi\varepsilon\varepsilon_0\left(\frac{k_B T}{ez}\right)^2 a\tanh^2\left(\frac{ez\psi_s}{4k_B T}\right)\exp(-\kappa(r-2a)) - \frac{aA_H}{12(r-2a)}. \quad (1)$$

z_i is the valence of the electrolyte in solution and e is the electron charge. A_H is the Hamaker constant that determines the magnitude of the attractive dispersion forces [57], k_B is Boltzmann's constant and T is the temperature. From Eq. 1, the energy is minimized when $r \to 2a$, or the particles come into contact and aggregate.

While an aggregated state is minimum in energy, for values of r of order κ^{-1}, the interaction energy (Eq. 1) can go through a local maximum, Φ_{max}. The rate of aggregation [58] decreases in the presence of such an energy barrier [59]. The ratio of the diffusion-limited flux, J_0, to the actual flux, J, which is known as the stability ratio, W, is proportional to the exponential of the maximum in the interaction energy, Φ_{max} [60]:

$$W = \frac{J_0}{J} \propto \exp\left[\frac{\Phi_{max}}{k_B T}\right]. \quad (2)$$

If Φ_{max} is large compared to the thermal energy, $k_B T$, W is large and the colloidal dispersion can be stabilized indefinitely against aggregation [28]. Eq. 2 also shows that any additive to the colloid dispersion that lowers Φ_{max} will destabilize the dispersion and lead to flocculation of the colloid [28]. Previous work has shown that Eq. 1 also governs the rate of adsorption of surfactant aggregates to an

albumin-covered interface (see [21] for details). As is the case for a stable colloidal dispersion, the presence of albumin at the interface creates a steric and electrostatic barrier that slows the rate of adsorption of surfactant to the interface. Under physiological conditions, $\Phi_{max} \sim 6\ k_B T$ for Survanta adsorption to an albumin covered interface [17] which, given the limited time (minutes) available for surfactant adsorption during expansion of the trough (or the much shorter times during normal respiration), effectively prevents sufficient surfactant from reaching the interface. Less surfactant at the interface requires greater compression ratios *in vitro* to reach a maximum surface pressure (see Fig. 1d); such compression ratios might not be achievable *in vivo*.

It follows that either increasing the attractive interactions or decreasing the repulsive interactions between surfactant and albumin should lower Φ_{max} and improve surfactant adsorption. Previous work [16,17,20,21,27] has shown that non-adsorbing hydrophilic polymers such as polyethylene glycol, dextran and hyaluronan enhance surfactant adsorption via increasing the attractive interactions between the surfactant and the interface via a depletion-attraction mechanism [41,42]:

$$\Phi_{dep} = -3(a/R_g)\phi_p k_B T\left[1-((r-2a)/2R_g)\right]^2 \quad (3)$$

R_g is the polymer radius of gyration and ϕ_p is the polymer volume fraction [41,42]. Eq. 3 adds an additional attractive term to Eq. 2, thereby decreasing Φ_{max}. The scaling of surfactant adsorption with polymer concentration [17] and molecular weight [20] verified the predictions of Eqs. 1–3. It is also possible to decrease the electrostatic repulsion (first term in Eq. 1) by increasing the electrolyte concentration in the suspension, thereby decreasing the Debye length, κ^{-1}, and hence the magnitude and range of the electrostatic repulsion [19,26]. Increasing the salt concentration from 150 mM to 1 M effectively restored surfactant adsorption in the presence of albumin [19]. As has been observed for nearly 100 years in studies of colloidal aggregation [61,62], surfactant adsorption was very sensitive to the valence, z, of the positively charged ions in solution.

The effects of chitosan, and by inference, other polycations, on surfactant adsorption also have direct analogies to colloidal stability. Polyelectrolytes are used to both stabilize and de-stabilize colloidal dispersions in wastewater treatment, mineral processing, ceramics manufacture and papermaking, and the origins of these effects have been extensively studied [30–35]. Adsorption of cationic polyelectrolytes to anionic colloids initially leads to a decrease of the overall net particle charge with a resulting decrease in the particle surface potential, ψ_s, in Eq. 1, thereby reducing Φ_{max}. At a certain polymer concentration, the net charge in the double-layer is neutralized, ψ_s and Φ_{max} in Eq. 1 go to zero, resulting in rapid aggregation [28]. However, with further increases in the polyelectrolyte concentration, the adsorption continues beyond net neutrality and leads to a charge reversal of the colloid, restoring ψ_s and Φ_{max}, leading to a re-stabilized colloidal dispersion [30–35].

The effects of polyelectrolytes on charge-stabilized colloids parallel those of the cationic chitosan on the adsorption of the anionic lung surfactant in the presence of anionic albumin: first an increase in adsorption at low chitosan concentrations, followed by a decrease in adsorption for higher chitosan concentrations (see. Figs. 2, 6). Polyelectrolytes, in general, adsorb to surfaces of opposite charge because the entropy increase caused by the release of the polymer and surface counter-ions to the solution; the positively charged amide groups on the chitosan can form ion pairs with oppositely charged ions on the surfactant and albumin surfaces, until the net charge in the electrical double layer is neutralized and the surface potential is reduced to zero (Eq. 1). However, this net neutralization cannot explain charge reversal; it is necessary to consider the details of the charge distribution of the surfaces and the polymers.

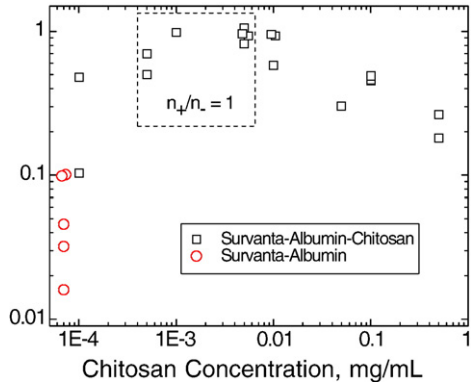

Fig. 6. Relative adsorption (RA) of 800 μg Survanta on subphases containing 2 mg/mL albumin at varying chitosan concentrations. □ Survanta–albumin–chitosan; ○ Survanta–albumin, which as been plotted at a chitosan concentration of $7\times10^{-}5$ mg/mL for comparison purposes. RA is the difference between the sample surface pressure (π) and the surface pressure of the albumin only isotherm (π_{Alb}, red curve in Fig. 1b), divided by the difference between the clean interface isotherm (no albumin), π_{Sat}, and π_{Alb}, $RA = \frac{\Pi-\Pi_{Alb}}{\Pi_{Sat}-\Pi_{Alb}}|_{A_0}$. All surface pressures were evaluated by averaging over the same trough area, A_0, denoted by the shaded area in Fig. 2. The relative adsorption increases with chitosan concentration to an optimum value of $RA \sim 1$ at .001–0.005 mg/mL chitosan and then decreases with subsequent increases in chitosan concentration. The dashed box indicates the calculated (Table 1) chitosan concentration range where $n^+/n^- = 1$ (0.0005–0.005 mg/mL). The optimum RA occurs in this chitosan concentration range consistent with a chitosan neutralizing the negative surface charge on the albumin and surfactant, thereby eliminating the electrostatic energy barrier to surfactant adsorption. Higher chitosan concentrations above $n^+/n^- = 1$ lead to charge reversal as excess chitosan adsorbs to the albumin and surfactant, leading to a net positive charge in the double layer and a restored energy barrier to adsorption (Eqs. 1–3).

In comparison to a solution of molecular ions like sodium or calcium, the positive charges on chitosan and other polyelectrolytes have a maximum and minimum separation fixed by the allowable polymer configurations. It is unlikely that the normal separations between negative charges in Survanta [63] or albumin are compatible with the separation between amide groups on the chitosan. Hence, a chitosan molecule with n^+ positive charges would not be capable of forming ion pairs with an equivalent number, n^-, of surface charges, as would be the case for n^+ individual sodium ions, for example. Hence, while n^+ positive charges on chitosan adsorbed to the surfactant or albumin can neutralize the average "smeared" net n^- negative charges in the double layer, resulting in a zero net potential in Eq. 1, the surface itself remains heterogeneous with patches of positive and negative charges [32,33]. Such a heterogeneous surface can lead to a short range "dipolar attraction" between the interfacial albumin and the surfactant bilayer aggregates, leading to a net attractive interaction between the surfactant and the interface. The can lead to enhanced adsorption even relative to a clean surface. In Fig. 2a, for chitosan concentration of .001 mg/mL, the amount of Survanta adsorbed to the interface in the presence of albumin is even greater than the control adsorption to a clean interface.

Additional chitosan can continue to adsorb as the polycation sees both attractive negative and repulsive positive charges on the surface while the net potential is low. The added chitosan can form ion pairs with the remaining negative charges on the surfactant or albumin surfaces. This over-compensation of charge is common; for example, certain polycations adsorb on net positively charged TiO_2 surfaces, where both positive and negative point charges coexist [35]. The result is a charge reversal as more positive ions are present in the vicinity of the surfaces than negative ions; chitosan continues to adsorb until the surfaces are sufficiently positively charged that the positively charged polymer is repelled from the surface by a now positive surface potential (Eq. 1) [33–35]. The net positively charged albumin and surfactant particles again have a repulsive interaction

with a new value of Φ_{max}, leading to a decreased rate of surfactant adsorption to the interface.

True equilibrium between the polycation and the anionic colloid is almost never obtained; polyelectrolyte adsorption is yet another case of kinetically hindered equilibrium. While each electrostatic ion pair between the polymer and the surface is weak, the large number possible between the polyelectrolyte (chitosan has ~500 cationic amine sites/molecule) and the negative charges makes the adsorption effectively irreversible [30,31,33,35]. Once bound, the polycation cannot readily adjust its position on the surface to neutralize the equivalent number of negative charges, especially if the charge distribution on the polymer does not match that on the surface. If the adjacent solution is diluted, the pH changed, etc., the polyelectrolyte does not necessarily desorb; there is a pronounced adsorption hysteresis that is typical for kinetically hindered equilibrium. This irreversibility of adsorption, combined with charge reversal makes possible the preparation of polyelectrolyte multilayers of anionic and cationic polymers on a variety of substrates including multilamellar liposomes [33].

Fig. 6 shows a quantitative demonstration of the effects of this chitosan-induced charge neutralization followed by charge overcompensation on the adsorption of lung surfactant to an albumin-covered interface. Since the area/molecule of Survanta is relatively constant at a given the surface pressure and temperature [49], the amount of surfactant adsorbed is proportional to the surface pressure at a fixed trough area [17]. Hence, the relative adsorption (RA) can be estimated to be the difference between the sample surface pressure (π) and the surface pressure of the albumin only isotherm (π_{Alb}, red curve in Fig. 1b), divided by the difference between the clean interface isotherm (no albumin), π_{Sat}, and π_{Alb}, $RA = \frac{\Pi - \Pi_{Alb}}{\Pi_{Sat} - \Pi_{Alb}}|_{A_0}$ [17,19,20]. All surface pressures were evaluated by averaging over the same trough area (A_0) denoted by the shaded area in Fig. 2b. This region showed the maximum variation in surface pressure. RA increases about 20 times as the chitosan concentration is increased from 0 to 0.005 mg/mL; subsequent increases in chitosan concentration result in roughly a five fold decrease in RA from the maximum. The optimal concentration range to enhance surfactant adsorption by chitosan ($RA \sim 1$) is 0.001–0.005 mg/mL. From Fig. 2a, surfactant adsorption is even greater at .001 mg/mL chitosan in the presence of albumin than on a clean interface.

Table 1 shows calculations for the ratio of the positive charges on chitosan relative to the negative charges on albumin and Survanta, n^+/n^-, as a function of chitosan concentration. Two limits of the charge ratio are considered: (1) comparing the total bulk concentrations of Survanta and albumin to chitosan (2) comparing the interfacial concentrations of Survanta and albumin to the bulk chitosan concentration. The 800 μg Survanta is spread near the interface; this amount of Survanta is scaled by the subphase volume (150 mL) and expanded trough area (130 cm^2) and to yield the bulk and interfacial concentrations. 2 mg/mL is used for the albumin bulk concentration while 5 mg/m^2 is used for the interfacial concentration [64]. For chitosan concentrations of 0.0005 and 0.005 mg/mL, the bulk and interfacial charge ratios bracket unity ($n^+/n^- = 1$). This concentration range is shown as the dashed box in Fig. 6, which should provide the greatest decrease in both ψ_s and Φ_{max}; the concentration range within the dashed box corresponds to the highest RA. This result is consistent with charge neutralization leading to enhance surfactant adsorption. The higher adsorption at .001 mg/mL chitosan is consistent with the formation of a heterogeneous surface with patches of positive and negative charges on the surfactant and albumin, which provide a dipolar attraction at close range. At higher chitosan concentrations, both the bulk and interfacial charge ratios in Table 1 show that the surfactant and albumin at the interface are net positively charged, resulting in a partially restored ψ_s and Φ_{max} and the albumin inhibition is only partially reversed. It should be noted that in our system, chitosan enhances surfactant adsorption ($RA > 0.2$) relative to albumin only subphases even at chitosan concentrations two orders of magnitude higher than charge neutralization, yielding a broad window of enhanced surfactant adsorption. A possible explanation for this behavior is that, from studies of alternate layer polyelectrolyte adsorption on surfaces, chitosan and other polyelectrolytes eventually saturate the surface and do not continuously increase the surface charge and surface potential with increasing bulk chitosan concentration [33,35]. Once the surfaces are saturated, the excess chitosan and counterions in solution reduces the Debye length, so that the electrostatic interactions due to the cationic polymers on the surfaces are shielded by the higher electrolyte concentration and resulting smaller Debye length (Eq. 1). This likely slows the decrease in surfactant adsorption with increasing chitosan concentration, just as we observed for higher electrolyte concentrations in previous work [19]. This optimal window of enhanced adsorption with the cation/anion charge ratio is almost identical to that reported for the stability ratio for chitosan induced flocculation of anionic colloidal particles [30–32].

The fluorescence images and the invariance of the Survanta isotherms with chitosan concentration on albumin containing subphases show that Survanta adsorption is enhanced without significant alteration of the Survanta interfacial properties. Albumin and Survanta appear immiscible in the fluorescence images; we observe a well-defined front of Survanta that displaces the albumin from the interface (Figs. 4, 5, and Supplemental Material). Zuo et al. [65] observed changes in bovine lung extract surfactant (BLES) film morphology and isotherms at low surface pressures which they ascribed to albumin and BLES film miscibility. Kang et al. [43] observed higher minimum surface tensions and changes in cyclic isotherms at high chitosan concentrations. The likely explanation for these differences is the much larger fraction of unsaturated lipids in BLES compared to Survanta [47], and the resulting larger fraction of liquid expanded (LE) phase in BLES monolayers compared to Survanta monolayers [49]. Polyelectrolytes interact strongly with LE films at low surface pressures, expanding the monolayer to larger area/molecule at a given surface pressure [66–69] through both electrostatic interactions with the head groups and hydrophobic interactions with the tail groups of the surfactant [68]. The extent of the modification of the LE phases correlates with the unsaturation of the fatty acid chains; saturated lipids that form LE phases only at lower surface pressures are less affected than are unsaturated lipids that have larger area/molecule and do not form LC phases until much higher surface

Table 1
Stenger et. al.

	Albumin	Chitosan	Survanta	
Molecular weight	66,430	120,000[a]	691[b]	
Charge/molecule	−2[c]	509[d]	−0.1[e]	
Chitosan: survanta + albumin: charge ratio				
Chitosan concentration, mg/mL	0.0005	0.005	0.05	0.5
n^+/n^- (Bulk)[f]	3.46×10^{-2}	0.346	3.46	34.6
n^+/n^- (Interface)[g]	2.69	26.9	2.69×10^{2}	2.69×10^{3}

For chitosan concentrations of 0.0005 and 0.005 mg/mL, the bulk and interfacial charge ratios bracket an estimate for $n^+/n^- = 1$ indicating charge neutralization occurs over this concentration range.

[a] Average molecular weight of chitosan, 50–190 kDa.

[b] Calculated molecular weight for DPPC:POPG:PA (70:20:10 wt.), a lipid mixture similar in composition to Survanta.

[c] Albumin charge/molecule at pH 5.5 in 150 mM NaCl [75].

[d] Calculated based on chitosan with average molecular weight of 120,000 with 80% of the monomers containing an amine group with pK_a of 6.5 at a pH of 5.5.

[e] Based on published Survanta composition showing ~10% anionic lipids [46].

[f] The charge ratio, n^+/n^-, of the cationic molecules (chitosan): anionic molecules (albumin and Survanta). For n^+/n^- bulk, the bulk concentrations of chitosan, albumin (2 mg/mL) and Survanta (800 μg/150 mL) are used.

[g] For n^+/n^- interface, the interfacial concentration of albumin (5 mg/m^2 [64]) and Survanta (800 μg/130 m^2) are compared with the bulk chitosan concentration.

pressures, if at all [69]. In addition to increasing the area/molecule in the LE phase, many polyelectrolytes, including chitosan, raise the collapse pressure of unsaturated fatty acid molecules from about 30 to 45 mN/m even though the limiting area/molecule at collapse increases from about 20 to 40 Å^2/molecule [67,69]. The chitosan is likely matching the minimum separation between charges along its backbone with the charge separation in the fatty acid films and the cross-linking of the headgroups via the chitosan stabilizes the monolayer against collapse, in a similar way as divalent ions increase the collapse pressure and stability of fatty acid films [67,70–74]. Hence, the chitosan (and other polyelectrolytes [67]) appear to help stabilize the LE phase in the monolayer. However, it is generally agreed that the unsaturated LE phase lipids must be "squeezed-out" in favor of the LC phase, saturated lipids that can reach the necessary lower surface tensions on compression [2]. If the unsaturated lipids in BLES films are not removed at low surface pressures, a higher fraction of LE phase may be retained in the monolayer film of BLES, which would then result in a less stable interfacial film and the films may collapse at the LE collapse pressure, which while increased by interactions with chitosan, is still not as high as the LC phase. As Survanta has very little LE phase at any surface pressure, chitosan would be expected to have a much smaller effect on Survanta, as we observe. The same explanation is likely true for the miscibility of albumin in the surfactant film. Zuo et al. [65] only observe albumin to be soluble in the LE phase; the small fraction of LE phase in Survanta at high surface pressures would cause complete exclusion of the albumin from the Survanta film and an immiscible displacement as is observed.

5. Conclusions

Chitosan, when added to the subphase, enhances the competitive adsorption of the clinical lung surfactant, Survanta, to an albumin-covered interface over a narrow concentration range. In direct analogy to chitosan's effects on anionic colloid stability, at the optimal concentration, the chitosan irreversibly adsorbs to the negatively charged albumin and Survanta, leading to a net neutralization of charge in the double layer and an elimination of the electrostatic barrier to Survanta adsorption. However, as the charge distribution on albumin, Survanta and chitosan are not perfectly matched, the albumin and Survanta surfaces, even at net neutrality, likely have patches of negative charge remaining on the surfaces that can bind additional chitosan. Hence, on addition of chitosan in excess of that needed to neutralize the surfaces, the net charge in the double layer is reversed, leading to a new positive surface potential and a new, likely different electrostatic barrier to Survanta adsorption, resulting in the decreased adsorption with increasing concentration that we see.

Every additive known to de-stabilize a charged colloidal suspension also enhances the competitive adsorption of Survanta: hydrophilic polymers that induce a depletion attraction [21], increased concentrations of molecular electrolytes that reduce the Debye length and screen the double-layer repulsion [19], and polycations that first neutralize the double-layer repulsion, then over compensate and re-stabilize the colloidal dispersion [33]. The simple analogy between colloid stability and competitive adsorption appears to be both qualitatively predictive and quantitatively accurate.

In addition to their generic effects on surfactant adsorption, albumin and chitosan can have specific effects that depend on surfactant composition and phase behavior. For Survanta, both albumin and chitosan have little effect on either isotherms or film morphology, once Survanta has displaced the albumin from the interface. The characteristic shoulder in the isotherm (that likely corresponds with unsaturated lipid squeeze-out) and monolayer collapse occur at the same surface pressure regardless of chitosan concentration or the presence of albumin in the subphase. Fluorescence images show the same Survanta morphology with chitosan and albumin in the subphase as for control Survanta on pure buffer. Survanta is immiscible with albumin and displaces the albumin from the interface at a well-defined boundary with little or no mixing. Other replacement surfactants, notably bovine lung extract surfactant, which has a higher fraction of unsaturated lipids and a greater range of liquid expanded phase, may be more miscible with albumin [65] and the LE phase behavior is altered by chitosan [43]. Survanta's ability to retain its high surface pressure at collapse and normal phase behavior in the presence of albumin and chitosan is likely due to the relatively small fraction of unsaturated lipids compared to BLES and may make Survanta performance more predictable in designing new treatments for ARDS.

Acknowledgements

We thank Bill Taeusch for ongoing collaborations on surfactant adsorption. Support for this work comes from National Institute of Health Grants HL-66410 (AJW), HL-51177 (JAZ), and the Tobacco Related Disease Research Program 14RT-0077 (JAZ, AJW). P.C.S. was partially supported by a NSF graduate research fellowship.

Appendix A. Supplementary data

Supplementary data associated with this article can be found, in the online version, at doi:10.1016/j.bbamem.2009.01.006.

References

[1] J.A. Clements, M.E. Avery, Lung surfactant and neonatal respiratory distress syndrome, Am. J. Respir. Crit. Care Med. 157 (1998) S59–S66.
[2] R. Notter, Lung Surfactant: Basic Science and Clinical Applications, Vol. 149, Marcel Dekker, New York, 2000.
[3] G.D. Rubenfeld, E. Caldwell, E. Peabody, J. Weaver, D.P. Martin, M. Neff, E.J. Stern, L.D. Hudson, Incidence and outcomes of acute lung injury, N. Engl. J. Med. 353 (2005) 1685–1693.
[4] J. Perez-Gil, Structure of pulmonary surfactant membranes and films: the role of proteins and lipid–protein interactions, Biochim. Biophys. Acta (BBA)-Biomembranes 1778 (2008) 1676–1695.
[5] R. Schmidt, P. Markart, C. Ruppert, M. Wygrecka, T. Kuchenbuch, D. Walmrath, W. Seeger, A. Guenther, Time-dependent changes in pulmonary surfactant function and composition in acute respiratory distress syndrome due to pneumonia or aspiration, Respir. Res. 8 (2007) 55.
[6] D.F. Willson, N.J. Thomas, B.P. Markovitz, L.A. Bauman, J.V. DiCarlo, S. Pon, B.R. Jacobs, L.S. Jefferson, M.R. Conaway, E.A. Egan, Effect of exogenous surfactant (calfactant) in pediatric acute lung injury, JAMA 293 (2005) 470–476.
[7] M. Duffett, K. Choong, V. Ng, A. Randolph, D.J. Cook, Surfactant therapy for acute respiratory failure in children: a systematic review and meta-analysis, Crit. Care 11 (2007).
[8] J.V. Been, L.J.I. Zimmermann, What's new in surfactant, Eur. J. Pediatr. 166 (2007) 889–899.
[9] J. Kesecioglu, J.J. Haitsma, Surfactant therapy in adults with acute lung injury/acute respiratory distress syndrome, Curr. Opin. Crit. Care 12 (2006) 55–60.
[10] R.G. Spragg, in: W.M. Zapol, F. Lemaire (Eds.), Adult Respiratory Distress Syndrome, Marcel Dekker, New York, 1991, pp. 381–395.
[11] A. Gunther, C. Ruppert, R. Schmidt, P. Markart, F. Grimminger, D. Walmrath, W. Seeger, Surfactant alteration and replacement in acute respiratory distress syndrome, Respir. Res. 2 (2001) 353-U2.
[12] A. Ishizaka, T. Matsuda, K.H. Albertine, H. Koh, S. Tasaka, N. Hasegawa, N. Kohno, T. Kotani, H. Morisaki, J. Takeda, M. Nakamura, X.H. Fang, T.R. Martin, M.A. Matthay, S. Hashimoto, Elevation of KL-6, a lung epithelial cell marker, in plasma and epithelial lining fluid in acute respiratory distress syndrome, Am. J. Physiol., Lung Cell. Mol. Physiol. 286 (2004) L1088–L1094.
[13] G. Nakos, E.I. Kitsiouli, I. Tsangaris, M.E. Lekka, Bronchoalveolar lavage fluid characteristics of early intermediate and late phases of ARDS — alterations in leukocytes, proteins, PAF and surfactant components, Intensive Care Med. 24 (1998) 296–303.
[14] B.A. Holm, G. Enhorning, R.H. Notter, A biophysical mechanism by which plasma-proteins inhibit lung surfactant activity, Chem. Phys. Lipids 49 (1988) 49–55.
[15] H.E. Warriner, J. Ding, A.J. Waring, J.A. Zasadzinski, A concentration-dependent mechanism by which serum albumin inactivates replacement lung surfactants, Biophys. J. 82 (2002) 835–842.
[16] H.W. Taeusch, J.B. de la Serna, J. Perez-Gil, C. Alonso, J.A. Zasadzinski, Inactivation of pulmonary surfactant due to serum-inhibited adsorption and reversal by hydrophilic polymers: experimental, Biophys. J. 89 (2005) 1769–1779.
[17] P.C. Stenger, J.A. Zasadzinski, Enhanced surfactant adsorption via polymer depletion forces: a simple model for reversing surfactant inhibition in acute respiratory distress syndrome, Biophys. J. 92 (2007) 3–9.

[18] J.J. Lu, W.W.Y. Cheung, L.M.Y. Yu, Z. Policova, D. Li, M.L. Hair, A.W. Neumann, The effect of dextran to restore the activity of pulmonary surfactant inhibited by albumin, Respir. Physiol. Neurobiol. 130 (2002) 169–179.
[19] P.C. Stenger, S.G. Isbell, D. St. Hilaire and J.A. Zasadzinski, Rediscovering the Schulz-Hardy Rule in Competitive Adsorption to an Air-Water Interace. Physical Review Letters (in review).
[20] P.C. Stenger, S.G. Isbell, J.A. Zasadzinski, Molecular weight dependence of the depletion attraction and its effects on the competitive adsorption of lung surfactant, Biochim. Biophys. Acta (BBA)-Biomembranes 1778 (2008) 2032–2040.
[21] J.A. Zasadzinski, T.F. Alig, C. Alonso, J.B. de la Serna, J. Perez-Gil, H.W. Taeusch, Inhibition of pulmonary surfactant adsorption by serum and the mechanisms of reversal by hydrophilic polymers: theory, Biophys. J. 89 (2005) 1621–1629.
[22] L. Gunasekara, W.M. Schoel, S. Schürch, M.W. Amrein, A comparative study of mechanisms of surfactant inhibition, Biochim. Biophys. Acta 1778 (2008) 433–444.
[23] K.W. Lu, H.W. Taeusch, B. Robertson, J. Goerke, J.A. Clements, Polyethylene glycol/surfactant mixtures improve lung function after HCl and endotoxin lung injuries, Am. J. Respir. Crit. Care Med. 164 (2001) 1531–1536.
[24] Y.Y. Zuo, H. Alolabi, A. Shafiei, N.X. Kang, Z. Policova, P.N. Cox, E. Acosta, M.L. Hair, A.W. Neumann, Chitosan enhances the in vitro surface activity of dilute lung surfactant preparations and resists albumin-induced inactivation, Pediatr. Res. 60 (2006) 125–130.
[25] A. Krishnan, J. Sturgeon, C.A. Siedlecki, E.A. Vogler, Scaled interfacial activity of proteins at the liquid–vapor interface, J. Biomed. Mater. Res. Part A 68A (2004) 544–557.
[26] T.F. Alig, H.E. Warriner, L. Lee, J.A. Zasadzinski, Electrostatic barrier to recovery of dipalmitoylphosphatidylglycerol monolayers after collapse, Biophys. J. 86 (2004) 897–904.
[27] L.M.Y. Yu, J.J. Lu, I.W.Y. Chiu, K.S. Leung, Y.W.W. Chan, L. Zhang, Z. Policova, M.L. Hair, A.W. Neumann, Poly(ethylene glycol) enhances the surface activity of a pulmonary surfactant, Colloids and Surf., B Biointerfaces 36 (2004) 167–176.
[28] W.B. Russel, D.A. Saville, W.R. Schowalter, Colloidal Dispersions, Cambridge University Press, Cambridge, 1989.
[29] P.C. Hiemenz, Principles of Colloid and Surface Chemistry, 2nd ed. Marcel Dekker, Inc., New York, 1986.
[30] M. Ashmore, J. Hearn, Flocculation of model latex particles by chitosans of varying degrees of acytlation, Lanmuir 16 (2000) 4906–4911.
[31] M. Ashmore, J. Hearn, F. Karpowicz, Flocculation of latex particles of varying surface charge densities by chitosan, Langmuir 17 (2001) 1069–1073.
[32] F. Bouyer, A. Robben, W.L. Yu, M. Borkovec, Aggregation of colloidal particles in the presence of oppositely charged polyelectrolytes: effect of surface charge heterogeneities, Langmuir 17 (2001) 5225–5231.
[33] G. Decher, Toward layered polymeric multicomposites, Science 277 (1997) 1232–1237.
[34] J. Kleimann, C. Gehin-Delval, H. Auweter, M. Borkovec, Super-stoichiometric charge neutralization in particle–polyelectrolyte systems, Langmuir 21 (2005) 3688–3698.
[35] K. Lowack, C.A. Helm, Molecular mechanisms controlling the self-assembly process of polyelectrolyte multilayers, Macromolecules 31 (1998) 823–833.
[36] T. Kobayashi, K. Ohta, K. Tashiro, K. Nishizuka, W.M. Chen, S. Ohmura, K. Yamamoto, Dextran restores albumin-inhibited surface activity of pulmonary surfactant extract, J. Appl. Physiol. 86 (1999) 1778–1784.
[37] K.W. Lu, H.W. Taeusch, B. Robertson, J. Goerke, J.A. Clements, Polymer-surfactant treatment of meconium-induced acute lung injury, Am. J. Respir. Crit. Care Med. 162 (2000) 623–628.
[38] H.W. Taeusch, K.W. Lu, J. Goerke, J.A. Clements, Nonionic polymers reverse inactivation of surfactant by meconium and other substances, Am. J. Respir. Crit. Care Med. 159 (1999) 1391–1395.
[39] K.W. Lu, J. Goerke, J.A. Clements, H.W. Taeusch, Hyaluronan decreases surfactant inactivation in vitro, Pediatr. Res. 57 (2005) 237–241.
[40] K.W. Lu, J. Goerke, J.A. Clements, H.W. Taeusch, Hyaluronan reduces surfactant inhibition and improves rat lung function after meconium injury, Pediatr. Res. 58 (2005) 206–210.
[41] P.D. Kaplan, J.L. Rouke, A.G. Yodh, D.J. Pine, Entropically driven surface phase-separation in binary colloidal mixtures, Phys. Rev. Lett. 72 (1994) 582–585.
[42] S. Asakura, F. Oosawa, Interactions between particles suspended in solutions of macromolecules, J. Polym. Sci. 33 (1958) 183–192.
[43] N.X. Kang, Z. Policova, G. Bankian, M.L. Hair, Y.Y. Zuo, A.W. Neumann, E.J. Acosta, Interaction between chitosan and bovine lung extract surfactants, Biochim. Biophys. Acta-Biomembranes 1778 (2008) 291–302.
[44] T. Bickel, Depletion forces near a soft surface, J. Chem. Phys. 118 (2003) 8960–8968.
[45] W. Bernhard, J. Mottaghian, A. Gebert, G.A. Rau, H. von der Hardt, C.F. Poets, Commercial versus native surfactants — surface activity, molecular components, and the effect of calcium, Am. J. Respir. Crit. Care Med. 162 (2000) 1524–1533.
[46] O. Blanco, J. Perez-Gil, Biochemical and pharmacological differences between preparations of exogenous natural surfactant used to treat respiratory distress syndrome: role of the different components in an efficient pulmonary surfactant, Eur. J. Pharmacol. 568 (2007) 1–15.
[47] A. Braun, P.C. Stenger, H.E. Warriner, J.A. Zasadzinski, K.W. Lu, H.W. Taeusch, A freeze-fracture transmission electron microscope and small angle X-ray diffraction study of the effects of albumin, serum and polymers on clinical lung surfactant microstructure, Biophys. J. 93 (2007) 123–139.
[48] F.J. Walther, L.M. Gordon, J.A. Zasadzinski, M.A. Sherman, A. Waring, Hydrophobic surfactant proteins and their analogues, Neonatology 91 (2007) 303–310.
[49] C. Alonso, T. Alig, J. Yoon, F. Bringezu, H. Warriner, J.A. Zasadzinski, More than a monolayer: relating lung surfactant structure and mechanics to composition, Biophys. J. 87 (2004) 4188–4202.
[50] M.M. Lipp, K.Y.C. Lee, A. Waring, J.A. Zasadzinski, Fluorescence, polarized fluorescence, and Brewster angle microscopy of palmitic acid and lung surfactant protein B monolayers, Biophys. J. 72 (1997) 2783–2804.
[51] J.A. Zasadzinski, J. Ding, H.E. Warriner, F. Bringezu, A.J. Waring, The physics and physiology of lung surfactants, Curr. Opin. Colloid Interface Sci. 6 (2001) 506–513.
[52] L. Pocivavsek, R. Dellsy, A. Kern, S. Johnson, B. Lin, K.Y.C. Lee, E. Cerda, Stress and fold localization in thin elastic membranes, Science 320 (2008) 912–916.
[53] J.Q. Ding, I. Doudevski, H.E. Warriner, T. Alig, J.A. Zasadzinski, Nanostructure changes in lung surfactant monolayers induced by interactions between palmitoyloleoylphosphatidylglycerol and surfactant protein B, Langmuir 19 (2003) 1539–1550.
[54] M. Shimojoh, K. Fukushima, K. Kurita, Low-molecular-weight chitosans derived from beta-chitin: preparation, molecular characteristics and aggregation activity, Carbohydr. Polym. 35 (1998) 223–231.
[55] F. Quemeneur, M. Rinaudo, B. Pepin-Donat, Influence of molecular weight and pH on adsorption of chitosan at the surface of large and giant vesicles, Biomacromolecules 9 (2008) 396–402.
[56] D. Marsh, Lateral pressure in membranes, Biochim. Biophys. Acta 1286 (1996) 183–223.
[57] J. Mahanty, B.W. Ninham, Dispersion Forces, Academic Press, New York, 1976.
[58] M.v. Smoluchowski, Versuch einer mathematischen Theorie def Koagulationkinetick Kollider Losungen, Z. Phys. Chem. 92 (1917) 129–168.
[59] N. Fuchs, Uber der stabilitat und aufladung der aerosole, Z. Phys. 89 (1934) 736–743.
[60] H. Reerinck, J.T.G. Overbeek, The rate of coagulation as a measure of hte stability of silver iodide sols, Disc. Far. Soc. 18 (1954) 74–84.
[61] H. Schulze, Schwefelarsen im wasseroger Losung, J. Prakt. Chem. 25 (1882) 431–452.
[62] W.B. Hardy, A preliminary investigation of the conditions which determine the stability of irreversible hydrosols, Proc. Roy. Soc. Lon. 66 (1900) 110–125.
[63] D.Y. Takamoto, M.M. Lipp, A. von Nahmen, K.Y.C. Lee, A.J. Waring, J.A. Zasadzinski, Interaction of lung surfactant proteins with anionic phospholipids, Biophys. J. 81 (2001) 153–169.
[64] S.J. McClellan, E.I. Franses, Effect of concentration and denaturation on adsorption and surface tension of bovine serum albumin, Colloids Surf. B Biointerfaces 28 (2003) 63–75.
[65] Y.Y. Zuo, S.M. Takayyon, E. Keating, L. Zhao, R.A.W. Veldhuizen, M.O. Peterson, M.W. Amrein, F. Possmayer, Atomic force microscopy studies of functional and dysfunctional pulmonary surfactant films: II. Albumin-inhibited pulmonary surfactant films and the effect of SP-A, Biophys. J. 95 (2008) 2779–2791.
[66] P.M. Bummer, S. Aziz, M.N. Gillespie, Inhibition of pulmonary surfactant biophysical activity by cationic polyamino acids, Pharm. Res. 12 (1995) 1658–1663.
[67] L.F. Chi, R.R. Johnston, H. Ringsdorf, Fluorescence microscopy investigations of the domain formation of fatty acid monolayers induced by polymeric gegenions, Langmuir 7 (1991) 2323–2329.
[68] F.J. Pavinatto, A. Pavinatto, L. Caseli, D.S. dos Santos, T.M. Nobre, M.E.D. Zaniquelli, O.N. Oliveira, Interaction of chitosan with cell membrane models at the air–water interface, Biomacromolecules 8 (2007) 1633–1640.
[69] P. Wydro, B. Krajewska, K. Hac-Wydro, Chitosan as a lipid binder: a Langmuir monolayer study of chitosan–lipid interactions, Biomacromolecules 8 (2007) 2611–2617.
[70] J.A. Zasadzinski, R. Viswanathan, L. Madsen, J. Garnaes, D.K. Schwartz, Langmuir–Blodgett Films, Science 263 (1994) 1726–1733.
[71] R. Viswanathan, L.L. Madsen, J.A. Zasadzinski, D.K. Schwartz, Liquid to hexatic to crystalline order in Langmuir–Blodgett films, Science 269 (1995) 51–54.
[72] D.Y. Takamoto, E. Aydil, J.A. Zasadzinski, A. Ivanova, D.K. Schwartz, T. Yang, P. Cremer, Stable ordering in Langmuir–Blodgett films, Science 293 (2001) 1292–1295.
[73] J. Garnaes, D.K. Schwartz, R. Viswanathan, J. Zasadzinski, Domain boundaries and buckling superstructures in Langmuir–Blodgett films, Nature 357 (1992) 54–57.
[74] M. Longo, A. Bisagno, J. Zasadzinski, R. Bruni, A. Waring, A function of lung surfactant protein SP-B, Science 261 (1993) 453–456.
[75] U. Bohme, U. Scheler, Effective charge of bovine serum albumin determined by electrophoresis NMR, Chem. Phys. Lett. 435 (2007) 342–345.